Deformation analysis of a geocell mattress using a decoupled iterative method

Ling Zhang[*], Minghua Zhao[a] and Heng Zhao[b]

College of Civil Engineering, Hunan University, 410082 Changsha, China

Abstract. Deformation analysis is a major concern in many geotechnical applications. In this paper, the deformation behavior of a geocell mattress subjected to symmetric loads was studied. The mattress was idealized as an elastic foundation beam. The horizontal beam-soil interfacial shear resistances at the beam top and bottom sides were taken into account by assuming the resistances to be linear with the relative horizontal displacements. A decoupled iterative method was employed to solve the differential displacement equations derived from the force analysis of a beam element and to obtain the solutions for the deformations and internal forces of the geocell reinforcement. The validity of the present solutions was verified by the existing finite element method and power-series solutions.

1. Introduction

A geocell is a three-dimensional interconnected geosynthetic material manufactured from different types of polymers. It has been increasingly applied in many geotechnical applications such as highway, railway and airport runway embankments because it can be used to improve base course properties by providing soil confinement to increase the soil stiffness and reduce deformations of the soil.

In the past decades, much attention has been focused on the reinforcement mechanism and bearing capacity of geocell reinforcements through experimental and numerical investigations (for example, Krishnaswamy *et al.* 2000, Dash *et al.* 2003, 2007, Latha *et al.* 2006, Zhou and Wen 2008, Zhang *et al.* 2010b). However, in some special cases, controlling the settlement of the superstructure is more important than increasing the foundation bearing capacity (Edgar *et al.* 1987, Xie *et al.* 2004, Han *et al.* 2007, Shahira and Pak 2010). Although settlement analysis is a major concern in many geotechnical applications, the number of studies in the literature that deal with deformation analyses of geocell mattresses is still limited.

According to existing studies, when analyzing the deformation behavior of a geocell-reinforced

---

∗Corresponding author, Ph.D., Research Associate, E-mail: zhanglhd@yahoo.com
[a]Professor, E-mail: mhzhaohd@21cn.com
[b]Ph.D., E-mail: tridept@163.com

mattress on a soft subgrade, the mattress can be regarded as a beam on elastic supports (Madhira and Hormoz 1988, Bourdeau 1989, Ghosh and Madhav 1994, Shukla and Chandra 1994, Yin 2000a, b, Maheshwari *et al*. 2006). Recent studies have demonstrated that the horizontal beam-soil interfacial shear resistance has a considerable influence on the behavior of the beam, especially when the foundation soil body is stiff and the contact face between the beam and the soil bed is rough (Tan 1997, Ma and Ai 2002). Several approaches have been proposed to evaluate the deformations of the foundation beam while considering the horizontal interfacial resistance effect. Two-parameter foundation models, such as the Filonenko-Borodich model (Filonenko-Borodich 1940) and Hetenyi model (Hetenyi 1946), are able to consider the horizontal interactions between the beam and the soil. In the Filonenko-Borodich and Hetenyi models, the horizontal tensile force along the beam is a constant. By using the conjugate beam method, an analogy for beam-foundation elastic systems was presented by Arici (1985). In the analogy (Arici 1985), the problem of an elastic beam on an elastic foundation was turned into an analogous problem of a conjugate beam on a conjugate foundation. Then, the beam was subjected to horizontal and vertical loads and imposed strains; the foundation reacted elastically both to the horizontal and vertical displacements and to the rotation. A partial solution for an infinite beam on an elastic foundation was proposed by Tan (1997). In his study, the foundation soil was idealized as horizontal and vertical springs. Closed-form solutions were obtained by Yin (2000a, b) to assess the performance of an infinite-reinforced Timoshenko beam. The beam in the study was subjected to a concentrated load in the mid-span and a uniform pressure loading at any location of the infinite beam. By using a finite element method (FEM), Ma and Ai (2002) discussed the effects of the horizontal beam-soil interfacial resistance on the behavior of the subgrade beam. By assuming different distribution patterns of the horizontal beam-soil interfacial resistance, Zhang *et al*. (2009, 2010a) developed power-series solutions to assess the performance of the geocell reinforcement while considering the influence of the interfacial resistance.

The purpose of this study is to develop solutions to assess the deformation of a geocell mattress with a decoupled iterative method. The mattress will be idealized as an elastic foundation beam. The differential equations with terms for the coupled horizontal and vertical displacements of the beam will be derived from a force analysis of a beam element. Moreover, it should be mentioned that the geocell products used to reinforce roadway and embankment often have different structures. The type of geocell with height of 100 mm~200 mm, weld distance of 400 mm, tensile strength more than 20 MPa, used normally in reinforcing of road subgrade, is suggested for the analytical model targeting in this study. The analytical model also is appropriate for the type of geocell which can make reinforced gravel mattress behaves as a stiffened platform.

2. Analytical model development

Only the case of symmetrical loads acting on the geocell mattress, as shown in Fig. 1, is analyzed in this study. In Fig. 1, $q(x)$ is a distributed load; P is an applied concentrated load; p_{ux} and p_{dx} are the horizontal interactions at the interfaces between the mattress and the soil above and below; p_z is the vertical subgrade reaction; l is the half length of the mattress; and h is the height of the mattress.

To simplify the problem, the following idealized conditions are assumed:

(1) The geocell mattress is modeled as an Euler-Bernoulli beam. Based on the basic hypotheses of the Euler-Bernoulli beam theory, the following relationships hold for an elastic beam
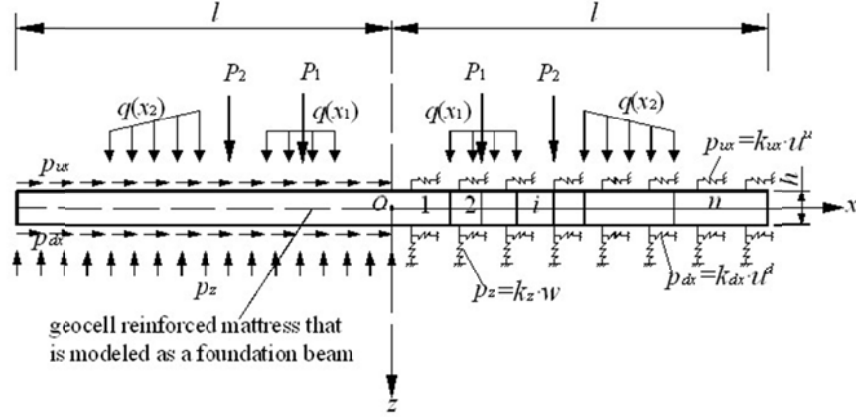
Fig. 1 A simplified calculation model of a geocell-reinforced mattress

$$
\begin{cases}
u(x,z) = u^0(x) - zw'(x) \\
\varepsilon_x(x,z) = (u^0)' - zw'' \\
\sigma_x(x,z) = E\varepsilon_x \\
T(x) = \int_A \sigma_x \mathrm{d}A = EA \cdot (u^0)' \\
M(x) = \int_A \sigma_x z \mathrm{d}A = -EIw'' \\
\theta(x) = w'
\end{cases}
\tag{1}
$$

where u and w are, respectively, the horizontal and vertical deformations of the beam; u^0 is the horizontal deformation on the neutral axis of the beam; and σ_x and ε_x are the stress and strain in the section of the beam, respectively; E is the equivalent elastic modulus of the beam, which depends on the geocell's type and size, the mattress composition and the unit weight of infilling materials, and its range can be varied from 30 MPa to 400 MPa (Hua 2003); The superscripts " ' " and " '' " denote the first-order and second-order partial derivatives with respect to x, respectively; T, M and θ are the tension force, bending moment and rotation angle of the beam, respectively; A is the cross-section area of the beam, $A = bh$; I is the inertia moment revolved around the neutral axis, $I = bh^3/12$; and b is the calculation width of the beam.

(2) If the subgrade soil is modeled as elastic Winkler springs, then

$$
p_z = k_z w
\tag{2}
$$

where k_z is the coefficient of vertical subgrade reaction.

(3) If the horizontal shear resistances at the top and bottom of the model beam are assumed to have linear relationships with the corresponding relative displacements, then
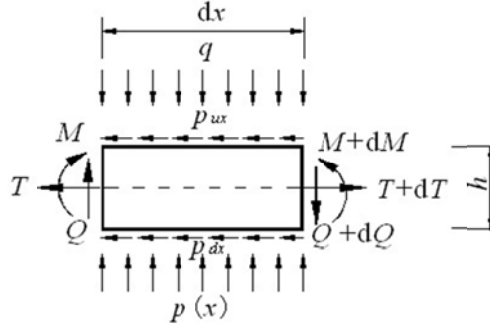
Fig. 2 Free-body diagram and forces

$$\begin{cases} p_{ux} = k_{ux} u^u \\ p_{dx} = k_{dx} u^d \end{cases} \tag{3}$$

where, u^u and u^d are the horizontal displacements at the top and bottom of the beam; and k_{ux} and k_{dx} are the corresponding soil coefficients. According to the first equation in equations set (1), u^u and u^d in Eq.(3) can be determined by $u^u = u^0 + h/2\, w'$ and $u^d = u^0 - h/2\, w'$, respectively. The values of the soil coefficients k_{ux}, k_{dx} and k_z can be evaluated on the basis of local experience, empirical relationships or site load testing (Bowles 1996). The units of k_{ux}, k_{dx} and k_z are kN/m^3 in this study.

The model beam is divided into n segments. One element from the ith segment on the right half ($x \geq 0$) of the beam, as shown in Fig. 2, is chosen for analysis. To simplify the analysis, a local coordinate system ξ_i-z with its origin o' at the mid-point of the left side of the ith segment is set up. Obviously, $\xi_i = x - \sum_{j=1}^{i-1} l_j$, where l_j is the length of the jth segment.

Applying force equilibrium to the element shown in Fig. 2, the following equations hold

$$\mathrm{d}T_i = b\left(p_{ux,i} + p_{dx,i} \right)\mathrm{d}\xi_i \tag{4}$$

$$\mathrm{d}Q_i = b\left[p_{z,i} - q_i \right]\mathrm{d}\xi_i \tag{5}$$

$$\mathrm{d}M_i = Q_i\mathrm{d}\xi_i - b\left(p_{ux,i} - p_{dx,i} \right)\frac{h}{2}\mathrm{d}\xi_i \tag{6}$$

Substituting the first and the fourth equations in equations set (1) and Eq. (3) into Eq. (4) yields the following equation

$$EA \cdot (u_i^0)'' - b\left(k_{ux} + k_{dx} \right)u_i^0 - \frac{bh}{2}\left(k_{ux} - k_{dx} \right)w_i' = 0 \tag{7}$$

Differentiating Eq. (6) and substituting Eqs. (1), (2), (3) and (5) into it leads to

$$EI \cdot w_i^{(4)} - \frac{b(k_{ux} + k_{dx})h^2}{4} \cdot w_i'' + bk_z w_i - bq_i - \frac{bh}{2}(k_{ux} - k_{dx}) \cdot (u_i^0)' = 0 \tag{8}$$

3. Determination of displacements *w* and *u*⁰

Eqs. (7) and (8) are the differential displacement equations with terms of coupled *w* and u^0. A decoupled iteration method is introduced to solve them with the following process:

(1) In the first step, the horizontal variables such as u^0, p_{ux}, p_{dx}, and *T* are neglected, and it is assumed that only the vertical displacement of the beam is generated under the vertical loads. Then, substituting $(u_i^0)' = 0$ into Eq. (8) and resolving the equation gives $w_i^{k=1}$. Then, $\theta_i^{k=1}$, $M_i^{k=1}$ and $Q_i^{k=1}$ are obtained.

(2) Substituting ($w_i^{k=1}$)′ as a constant into Eq. (7) yields $(u_i^0)^{k=1}$. Then, $\left((u_i^0)^{k=1}\right)'$ is obtained.

(3) Substituting $\left((u_i^0)^{k=1}\right)'$ as a constant into Eq. (8) gives $w_i^{k=2}$. Then, $\theta_i^{k=2}$, $M_i^{k=2}$ and $Q_i^{k=2}$ are obtained.

(4) The rest of the steps may be deduced by analogy until the following inequalities

$$\begin{cases} \left| \dfrac{w_i^k - w_i^{k-1}}{w_i^k} \right| < \zeta \\[4mm] \left| \dfrac{(u_i^0)^k - (u^0)^{k-1}}{(u_i^0)^k} \right| < \zeta \end{cases} \tag{9}$$

are satisfied for all *i* (*i* =1,…,*n*), where ζ is a specified tolerance, which is considered to be 10^{-6} in this study.

The detailed calculation process to obtain the variables w_i^k, θ_i^k, M_i^k, Q_i^k, $(u_i^0)^k$ and T_i^k in the *k*th iterative step is presented in the following sections.

3.1 Determination of vertical displacement w

Eq. (8) in the *k*th iterative step can be written as

$$EI \cdot \left(w_i^k\right)^{(4)} - X_i \cdot \left(w_i^k\right)'' + bk_z w_i^k = Y_i^{k-1} \tag{10}$$

with

$$X_i = \frac{bh^2}{4}(k_{ux} + k_{dx}); \text{ and } Y_i^{k-1} = bq_i + \frac{bh}{2}(k_{ux} - k_{dx}) \cdot \left((u_i^0)^{k-1}\right)' \tag{11}$$

the superscript k means that the values of the variables are obtained in the kth step; and the superscript (k-1) means that the values of the variables can be obtained in the (k-1)th step. When k=1, $\left((u_i^0)^{k-1}\right)' = 0$.

For practical simplifications, only linearly varying distributed loadings need be considered. Then, the distributed load q_i in Eq. (8) that acts on the ith segment can be expressed as follows:

$$q_i = g_i\xi_i + d_i \tag{12}$$

where g_i and d_i are constants. For a uniformly distributed load, g_i=0 and $d_i \neq 0$, but for a triangularly distributed load, $g_i \neq 0$ and $d_i \neq 0$.

When $(u_i^0)'$ is regarded as a constant, the solution of Eq. (8) is

$$w_i^k = A_i^k f_{A,i} + B_i^k f_{B,i} + C_i^k f_{C,i} + D_i^k f_{D,i} + \frac{Y_i^{k-1}}{bk_z} \tag{13}$$

where A_i^k, B_i^k, C_i^k and D_i^k are four unknown coefficients; and $f_{A,i}$, $f_{B,i}$, $f_{C,i}$, and $f_{D,i}$ are constants defined as

$$f_{A,i} = \begin{cases} e^{\alpha_i\xi_i}\cos(\beta_i\xi_i), & \Delta_i < 0 \\ e^{r_{A,i}\xi_i}, & \Delta_i \geq 0 \text{ and } X_i \geq 0 \\ \cos(\varphi_{1,i}\xi_i), & \Delta_i \geq 0 \text{ and } X_i < 0 \end{cases} \tag{14}$$

$$f_{B,i} = \begin{cases} e^{\alpha_i\xi_i}\sin(\beta_i\xi_i), & \Delta_i < 0 \\ e^{r_{B,i}\xi_i}, & \Delta_i \geq 0 \text{ and } X_i \geq 0 \\ \sin(\varphi_{1,i}\xi_i), & \Delta_i \geq 0 \text{ and } X_i < 0 \end{cases} \tag{15}$$

$$f_{C,i} = \begin{cases} e^{-\alpha_i\xi_i}\cos(\beta_i\xi_i), & \Delta_i < 0 \\ e^{r_{C,i}\xi_i}, & \Delta_i \geq 0, \ X_i \geq 0 \\ \cos(\varphi_{2,i}\xi_i), & \Delta_i \geq 0, \ X_i < 0 \end{cases} \tag{16}$$

$$f_{D,i} = \begin{cases} e^{-\alpha_i\xi_i}\sin(\beta_i\xi_i), & \Delta_i < 0 \\ e^{r_{D,i}\xi_i}, & \Delta_i \geq 0 \text{ and } X_i \geq 0 \\ \sin(\varphi_{2,i}\xi_i), & \Delta_i \geq 0 \text{ and } X_i < 0 \end{cases} \tag{17}$$

where $\alpha_i = \dfrac{\sqrt{\sqrt{\dfrac{4bk_z}{EI}} + \dfrac{X_i}{EI}}}{2}$; $\beta_i = \dfrac{\sqrt{\sqrt{\dfrac{4bk_z}{EI}} - \dfrac{X_i}{EI}}}{2}$; $r_{A,i} = \sqrt{\dfrac{\dfrac{X_i}{EI} + \sqrt{\Delta_i}}{2}}$; $r_{B,i} = -\sqrt{\dfrac{\dfrac{X_i}{EI} + \sqrt{\Delta_i}}{2}}$;

$r_{C,i} = \sqrt{\dfrac{\dfrac{X_i}{EI} - \sqrt{\Delta_i}}{2}}$; $r_{D,i} = -\sqrt{\dfrac{\dfrac{X_i}{EI} - \sqrt{\Delta_i}}{2}}$; $\varphi_{1,i} = \sqrt{\dfrac{-\dfrac{X_i}{EI} - \sqrt{\Delta_i}}{2}}$; $\varphi_{2,i} = \sqrt{\dfrac{-\dfrac{X_i}{EI} + \sqrt{\Delta_i}}{2}}$; and

$\Delta_i = \left(\dfrac{X_i}{EI}\right)^2 - \dfrac{4bk_z}{EI}$.

Then, the rotational angle θ, bending moment M and shear force Q of the ith beam segment can be expressed as

$$
\begin{cases}
\theta_i^k = (w_i^k)' = A_i^k (f_{A,i})' + B_i^k (f_{B,i})' + C_i^k (f_{C,i})' + D_i^k (f_{D,i})' + \dfrac{(Y_i^{k-1})'}{bk_z} \\[2mm]
M_i^k = -EI(w_i^k)'' = -EI \cdot \left[A_i^k (f_{A,i})'' + B_i^k (f_{B,i})'' + C_i^k (f_{C,i})'' + D_i^k (f_{D,i})'' + \dfrac{(Y_i^{k-1})''}{bk_z} \right] \\[3mm]
Q_i^k = -EI(w_i^k)''' + \left(p_{ux,i}^{k-1} - p_{dx,i}^{k-1} \right)\dfrac{bh}{2} + T_i^{k-1}(w_i^k)' \\[2mm]
\quad = -EI(w_i^k)''' + X_i(w_i^k)' + \dfrac{b(k_{ux} - k_{dx})h}{2}(u_i^0)^{k-1} \\[2mm]
\quad = (\overline{f}_{A,i})''' A_i^k + (\overline{f}_{B,i})''' B_i^k + (\overline{f}_{C,i})''' C_i^k + (\overline{f}_{D,i})''' D_i^k + \dfrac{X_i(Y_i^{k-1})'}{bk_z} + \dfrac{bh}{2}(k_{ux} - k_{dx})(u_i^0)^{k-1}
\end{cases}
\tag{18}
$$

where

$$
(\overline{f}_{j,i})''' = -EI(f_{j,i})''' + X_i(f_{j,i})'
\tag{19}
$$

and the subscripts $j = A, B, C, D$.

Eqs. (13) and (18) can be written into a matrix format as follows

$$
\begin{bmatrix} w_i^k \\ \theta_i^k \\ M_i^k \\ Q_i^k \end{bmatrix} = \boldsymbol{F}_i \cdot \begin{bmatrix} A_i^k \\ B_i^k \\ C_i^k \\ D_i^k \end{bmatrix} + \boldsymbol{\Lambda}_i^k
\tag{20}
$$

with

$$\boldsymbol{F}_i = \begin{bmatrix} f_{A,i} & f_{B,i} & f_{C,i} & f_{D,i} \\ (f_{A,i})' & (f_{B,i})' & (f_{C,i})' & (f_{D,i})' \\ -EI(f_{A,i})'' & -EI(f_{B,i})'' & -EI(f_{C,i})'' & -EI(f_{D,i})'' \\ (\overline{f}_{A,i})''' & (\overline{f}_{B,i})''' & (\overline{f}_{C,i})''' & (\overline{f}_{D,i})''' \end{bmatrix} \tag{21}$$

and

$$\boldsymbol{\Lambda}_i^k = \frac{1}{k_z} \cdot \begin{bmatrix} (Y_i^{k-1}) \\ (Y_i^{k-1})' \\ 0 \\ X_i(Y_i^{k-1})' + \dfrac{bhk_z}{2}(k_{ux} - k_{dx})(u_i^0)^{k-1} \end{bmatrix} \tag{22}$$

Substituting $\xi_i=0$ into Eq. (20), the four unknown coefficients A_i^k, B_i^k, C_i^k and D_i^k in the above Eqs. (13) and (18) can be determined by

$$\begin{bmatrix} A_i^k \\ B_i^k \\ C_i^k \\ D_i^k \end{bmatrix} = \left[\boldsymbol{F}_i \big|_{\xi_i=0} \right]^{-1} \left(\begin{bmatrix} w_{i,0}^k \\ \theta_{i,0}^k \\ M_{i,0}^k \\ Q_{i,0}^k \end{bmatrix} - \boldsymbol{\Lambda}_i^k \big|_{\xi_i=0} \right) \tag{23}$$

where $w_{i,0}^k, \theta_{i,0}^k, M_{i,0}^k$ and $Q_{i,0}^k$ are the vertical deformation, rotation angle, bending moment and shear force at $\xi_i=0$ in the kth iterative step, respectively.

Substituting Eq. (23) into Eq. (20) gives

$$\begin{bmatrix} w_i^k \\ \theta_i^k \\ M_i^k \\ Q_i^k \end{bmatrix} = \boldsymbol{FF}_i \cdot \begin{bmatrix} w_{i,0}^k \\ \theta_{i,0}^k \\ M_{i,0}^k \\ Q_{i,0}^k \end{bmatrix} + \boldsymbol{\Lambda\Lambda}_i^k \tag{24}$$

with

$$\boldsymbol{FF}_i = \boldsymbol{F}_i \cdot \left[\boldsymbol{F}_i \big|_{\xi_i=0} \right]^{-1}; \quad \boldsymbol{\Lambda\Lambda}_i^k = -\boldsymbol{FF}_i \cdot \boldsymbol{\Lambda}_i^k \big|_{\xi_i=0} + \boldsymbol{\Lambda}_i^k \tag{25}$$

By substituting the continuity conditions

$$\begin{cases} w_{i,0}^k = w_{i-1,l_{i-1}}^k \\ \theta_{i,0}^k = \theta_{i-1,l_{i-1}}^k \\ M_{i,0}^k = M_{i-1,l_{i-1}}^k \\ Q_{i,0}^k = Q_{i-1,l_{i-1}}^k - P_{i,i-1} \end{cases} \tag{26}$$

at the point $x = \sum_{j=1}^{i-1} l_j$ into Eq.(24), then, by analogy, the vertical deformation, rotation angle, bending moment and shear force w_i^k, θ_i^k, M_i^k and Q_i^k can be expressed by the corresponding variables w_0, θ_0, M_0 and Q_0 at the beam center ($x=0$).

$$\begin{bmatrix} w_i^k \\ \theta_i^k \\ M_i^k \\ Q_i^k \end{bmatrix} = FF_i \cdot \overline{FF}_{i-1} \cdot \overline{FF}_{i-2} \cdots \overline{FF}_1 \cdot \begin{bmatrix} w_0^k \\ \theta_0^k \\ M_0^k \\ Q_0^k \end{bmatrix} \tag{27}$$

$$+ \left(FF_i \cdot \left(\overline{FF}_{i-1} \cdot \left(\overline{FF}_{i-2} \cdot \left(\dots \left(\overline{FF}_2 \cdot \overline{AP}_1^k + \overline{AP}_2^k \right) \dots \right) + \overline{AP}_{i-2}^k \right) + \overline{AP}_{i-1}^k \right) + AA_i^k \right)$$

with

$$\overline{FF}_{i-1} = FF_{i-1}\big|_{\xi_{i-1}=l_{i-1}} ; \quad \overline{AP}_{i-1}^k = AP_{i-1}^k\big|_{\xi_{i-1}=l_{i-1}} ; \quad AP_{i-1}^k = AA_{i-1}^k - \begin{bmatrix} 0 \\ 0 \\ 0 \\ P_{i,i-1} \end{bmatrix} \tag{28}$$

where, $P_{i,i-1}$ is the concentrated load acting at the point $x = \sum_{j=1}^{i-1} l_j$; if there is no concentrated load acting at the point, $P_{i,i-1} = 0$; and w_0, θ_0, M_0 and Q_0 can be determined by boundary conditions. Taking a beam with free ends and subjected to symmetric loads for example, the following boundary conditions exist

$$\text{(a)} \begin{cases} \theta\big|_{x=0} = 0 \\ Q\big|_{x=0} = -P_0/2 \end{cases} \text{and (b)} \begin{cases} M\big|_{x=l} = 0 \\ Q\big|_{x=l} = 0 \end{cases} \tag{29}$$

where P_0 is the concentrated load acting at the point $x=0$. The boundary conditions in group (a) are from the symmetry of the beam, and those in group (b) are due to the free ends of the beam.

3.2 Determination of horizontal displacement u^0

Eq. (7) in the kth iterative step can be written as

$$EA\left((u_i^0)^k\right)'' - b\left(k_{ux} + k_{dx}\right)(u_i^0)^k = \frac{bh}{2}\left(k_{ux} - k_{dx}\right)(w_i^k)' \tag{30}$$

When $(w_i^k)'$ in the equation is regarded as a constant in calculation, the solution of Eq. (30) is

$$(u_i^0)^k = c_{i,1}^k e^{a\xi_i} + c_{i,2}^k e^{-a\xi_i} + \varpi_i^k \tag{31}$$

with

$$a = \sqrt{\frac{b\left(k_{ux} + k_{dx}\right)}{EA}} \ ; \quad \varpi_i^k = -\frac{h\left(k_{ux} - k_{dx}\right) \cdot (w_i^k)'}{2\left(k_{ux} + k_{dx}\right)} \tag{32}$$

$c_{i,1}^k$ and $c_{i,2}^k$ in Eq.(31) are two unknown coefficients.

Then, the tension force T_i^k is

$$T_i^k = EA\left((u_i^0)^k\right)' = EAa \cdot \left(c_{i,1}^k e^{a\xi_i} - c_{i,2}^k e^{-a\xi_i}\right) \tag{33}$$

Similar to Eqs. (18) to (27), Eqs. (31) and (33) can be written into a matrix format as follows

$$\begin{bmatrix} (u_i^0)^k \\ \dfrac{T_i^k}{EA} \end{bmatrix} = \begin{bmatrix} \text{ch}(a\xi_i) & \dfrac{\text{sh}(a\xi_i)}{a} \\ a \cdot \text{sh}(a\xi_i) & \text{ch}(a - \xi_i) \end{bmatrix} \begin{bmatrix} (u_{i,0}^0)^k \\ \dfrac{T_{i,0}^k}{EA} \end{bmatrix} - \begin{bmatrix} \text{ch}(a\xi_i) - 1 & \dfrac{\text{sh}(a\xi_i)}{a} \\ a \cdot \text{sh}(a\xi_i) - 1 & \text{ch}(a\xi_i) \end{bmatrix} \cdot \begin{bmatrix} \varpi_i^k \\ 0 \end{bmatrix} \tag{34}$$

where $(u_{i,0}^0)^k$ and $T_{i,0}^k$ are the horizontal deformation on the neutral axis of the beam and the tension force within the beam at $\xi_i=0$ in the kth iterative step, respectively. Obviously, a in Eq. (34) cannot be zero, so k_{ux} and k_{dx} cannot both be zero at the same time. In the calculation, if $k_{ux} = k_{dx} = 0$, $k_{ux} = k_{dx}+\delta$, where δ is an assumed constant with an extremely small value.

Combining with the continuity conditions

$$\begin{cases} (u_{i,0}^0)^k = (u_{i-1,l_{i-1}}^0)^k \\ T_{i,0}^k = T_{i-1,l_{i-1}}^k \end{cases} \tag{35}$$

at the point $x = \sum\limits_{j=1}^{i-1} l_j$, the following matrix equation can be obtained by analogy:

$$\begin{bmatrix} (u_i^0)^k \\ \dfrac{T_i^k}{EA} \end{bmatrix} = \boldsymbol{S}_i \cdot \overline{\boldsymbol{S}}_{i-1} \cdot \overline{\boldsymbol{S}}_{i-2} \cdot ... \overline{\boldsymbol{S}}_1 \cdot \begin{bmatrix} (u_0^0)^k \\ \dfrac{T_0^k}{EA} \end{bmatrix}$$
$$+ \left(\boldsymbol{S}_i \cdot \left(\overline{\boldsymbol{S}}_{i-1} \cdot \left(\overline{\boldsymbol{S}}_{i-2} \cdot \left(... \left(\overline{\boldsymbol{S}}_2 \cdot \overline{\boldsymbol{W}}_1^k + \overline{\boldsymbol{W}}_2^k \right) ... \right) + \overline{\boldsymbol{W}}_{i-2}^k \right) + \overline{\boldsymbol{W}}_{i-1}^k \right) + \boldsymbol{W}_i^k \right) \tag{36}$$

with

$$\overline{\boldsymbol{S}}_{i-1} = \boldsymbol{S}_{i-1} \Big|_{\xi_{i-1}=l_{i-1}} ; \quad \boldsymbol{S}_i = \begin{bmatrix} \mathrm{ch}(a\xi_i) & \dfrac{\mathrm{sh}(a\xi_i)}{a} \\ a \cdot \mathrm{sh}(a\xi_i) & \mathrm{ch}(a\xi_i) \end{bmatrix} \tag{37}$$

$$\overline{\boldsymbol{W}}_{i-1}^k = \boldsymbol{W}_{i-1}^k \Big|_{\xi_{i-1}=l_{i-1}} ; \quad \boldsymbol{W}_i^k = -\begin{bmatrix} \mathrm{ch}(a\xi_i)-1 & \dfrac{\mathrm{sh}(a\xi_i)}{a} \\ a \cdot \mathrm{sh}(a\xi_i)-1 & \mathrm{ch}(a\xi_i) \end{bmatrix} \cdot \begin{bmatrix} \varpi_i^k \\ 0 \end{bmatrix} \tag{38}$$

u_0^0 and T_0 in Eq.(36) are, respectively, the horizontal deformation and tension force at the beam center (x=0), which can be determined by boundary conditions. For a free-ends beam subjected to symmetric loads, the following boundary conditions exist

$$\begin{cases} u^0 \big|_{x=0} = 0 \\ T \big|_{x=l} = 0 \end{cases} \tag{39}$$

Table 1 Comparison of node deflections (k_z=5×10³ kN/m³) (Unit: mm)

Calculation methods	A	B	C	D	E
FEM (Ma and Ai 2002)	13.18	13.68	13.61	17.99	16.62
Power-series solutions (Zhang *et al.* 2010a)	12.90	13.64	14.69	16.74	16.77
Current solutions	12.88	13.65	14.69	16.74	16.77

Notice: the placements of nodes "A, B, C, D, and E" are shown in Fig. 3

Table 2 Comparison of node shear forces (k_z=5×10³ kN/m³) (Unit: kN)

Calculation methods	A	B$^{\text{left}}$	B$^{\text{right}}$	C	D$^{\text{left}}$	D$^{\text{right}}$	E
FEM (Ma and Ai 2002)	0	506.5	-715.5	83.6	1034.6	-1041.4	0
Power-series solutions (Zhang *et al.* 2010a)	0	498.1	-723.9	120.7	1066.2	-1009.8	0
Current solutions	0	498.1	-723.9	120.8	1066.2	-1009.8	0

Notice: (1) the placements of nodes "A, B, C, D, and E" are shown in Fig. 3
(2) B$^{\text{left}}$ and B$^{\text{right}}$ are the shear forces on the left- and right- section of the point B=0, respectively
D$^{\text{left}}$ and D$^{\text{right}}$ are the shear forces on the left- and right- section of the point D=0, respectively

Table 3 Comparison of node bending moments (k_z=5×10³ kN/m³) (Unit: kN·m)

Calculation methods	A	B	C	D	E
FEM (Ma and Ai 2002)	0	626.6	-629.5	1487.0	-552.3
Power-series solutions (Zhang *et al.* 2010a)	0	612.5	-619.0	1700.0	-318.2
Current solutions	0	612.5	-618.9	1700.0	-318.1

Notice: the placements of nodes "A, B, C, D, and E" are shown in Fig. 3

Table 4 Comparison of node deformations (k_z=30×10³ kN/m³) (Unit: mm)

Calculation methods	A	B	C	D	E
FEM (Ma and Ai 2002)	2.16	2.55	1.60	3.76	2.20
Power-series solutions (Zhang *et al.* 2010a)	2.22	2.31	2.20	3.09	2.70
Current solutions	2.22	2.31	2.20	3.10	2.71

Notice: the placements of nodes "A, B, C, D, and E" are shown in Fig. 3

Table 5 Comparison of node shear forces (k_z=30×10³ kN/m³) (Unit: kN)

Calculation methods	A	B^{left}	B^{right}	C	D^{left}	D^{right}	E
FEM (Ma and Ai 2002)	0	544.3	-677.7	36.1	1022.7	-1053.3	0
Power-series solutions (Zhang *et al.* 2010a)	0	514.1	-707.9	78.1	1032.5	-1043.5	0
Current solutions	0	515.1	-708.9	79.5	1033.4	-1042.6	0

Notice: (1) the placements of nodes "A, B, C, D, and E" are shown in Fig. 3;
(2) B^{left} and B^{right} are the shear forces on the left- and right- section of the point B=0, respectively
D^{left} and D^{right} are the shear forces on the left- and right- section of the point D=0, respectively

Table 6 Comparison of node bending moments (k_z=30×10³ kN/m³) (Unit: kN·m)

Calculation methods	A	B	C	D	E
FEM (Ma and Ai 2002)	0	614.6	-405.4	1174	-476.8
Power-series solutions (Zhang *et al.* 2010a)	0	631.5	-575.6	1406.7	-560.1
Current solutions	0	630.5	-578.6	1410.7	-558.4

Notice: the placements of nodes "A, B, C, D, and E" are shown in Fig. 3

4. Validation

In order to make a comparative verification of the current solutions, the same foundation beam with length of 29.0 m, width of 3.0 m, height of 1.0 m and elastic modulus 20.5 × 10³ MPa studied by Ma and Ai (2002) was employed in the analysis. The beam was subjected to symmetric concentrated loads, as shown in Fig. 3. The behaviors of the beam on both soft and stiff soil beds had already been assessed by the finite element method (FEM) developed by Ma and Ai (2002) and their results were also employed for comparison. The power-series semi-analytic solutions proposed by Zhang *et al.* (2010a) were also employed to assess the behaviors of the beam on different soil beds for comparison. In the calculation, the values of soil parameters were chosen the same as those in Ma and Ai's study as follows: horizontal soil reaction k_{dx} = 7.5 × 10³ kN/m³ for soft soil and k_{dx} = 200 × 10³ kN/m³ for stiff soil; coefficient of vertical soil reaction k_z = 5 × 10³ kN/m³ for soft soil and k_z = 30×10³ kN/m³ for stiff soil.
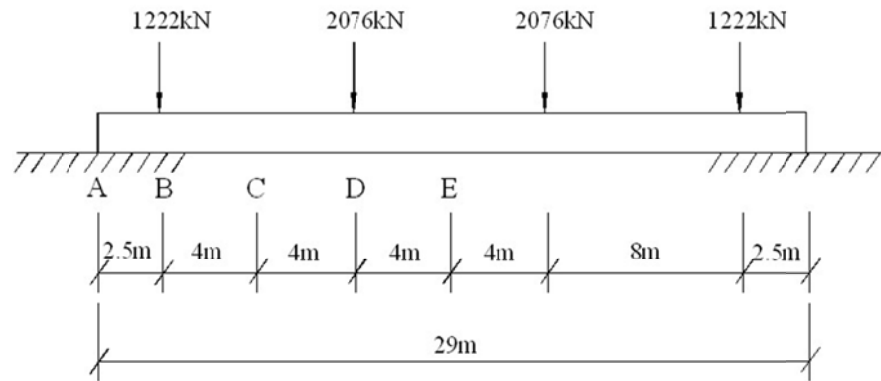
Fig. 3 Elastic foundation beam with applied loads

Because the horizontal beam-soil interaction only existed at the interface between the beam and the soil below in Ma and Ai's study, the value of the horizontal foundation coefficient above the foundation beam k_{ux} is chosen to be 0 kN/m^3 in the calculation. Comparisons of the node displacements, shear forces and moments derived from the current method with those from the FEM method and the power-series solutions are shown in Tables 1-6. It can be seen that the results derived from the current method match the results from the FEM method (Ma and Ai 2002) most closely and are almost the same as the results from the power-series solutions (Zhang *et al.* 2010a).

5. Parameter study

A hypothetical geocell-reinforced embankment (shown in Fig. 4) was set up for a parameter study. The embankment fill is 1.5 m high and 7.0 m wide at the surface with a unit weight of 20 kN/m^3, the side slope of the embankment is 2H:1V. Symmetrical concentrated loads $P_1=P_2=250$ kN are acting on the embankment surface. The locations of P_1 and P_2 are also shown in Fig. 4. A geocell reinforced gravel mattress with height 0.5 m and transverse width 15m is located under the embankment fill.

In the analysis, the geocell reinforced mattress was treated as an elastic foundation beam; the weight of the embankment fill was treated as the distributed load acting on the beam. Due to embankment symmetry, only the right half of the geocell reinforced mattress was analyzed. Because the length of the embankment is much larger than its width, only the unit longitudinal wide of the embankment was chosen to analysis, i.e., $b=1.0$ m. From the above derivation, if dimensions of embankment and mattress, and external loads keep constants, the behavior of the beam is related to the horizontal and vertical soil reactions, k_{dx}, k_{ux} and k_z, and the equivalent elastic modulus of the beam E. In the parametric study, k_z is varied from 5000 kN/m^3 to 10000 kN/m^3, $k_{dx}=k_z$, k_{ux} is varied from $2k_{dx}$ to $4k_{dx}$, E is varied from 50MPa, 150MPa to 300MPa. Then, nine cases with different values of k_z, k_{ux}/k_{dx}, and E were summarized in Table 7.

The proposed iterative method was used to assess the behavior of the geocell reinforcement problem shown in Fig. 4. The predicted vertical deformation w and tension force T within the beam were shown in Figs. 5 to 6. From Figs. 5 to 6, it can be observed that when other calculation parameters keep constants, the maximum vertical deformation w_{max} decreases with E increases,
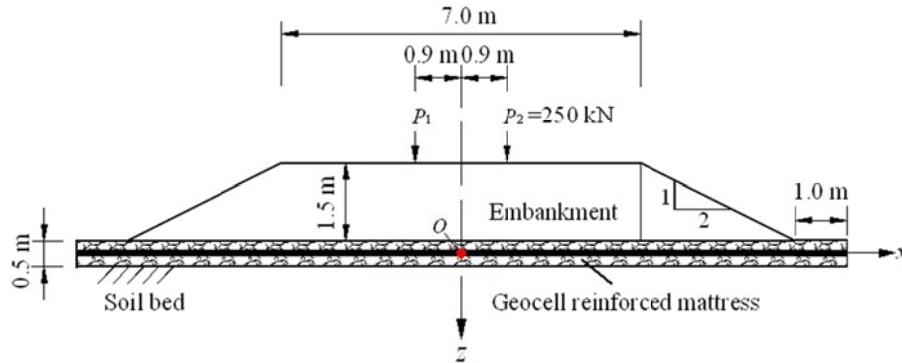
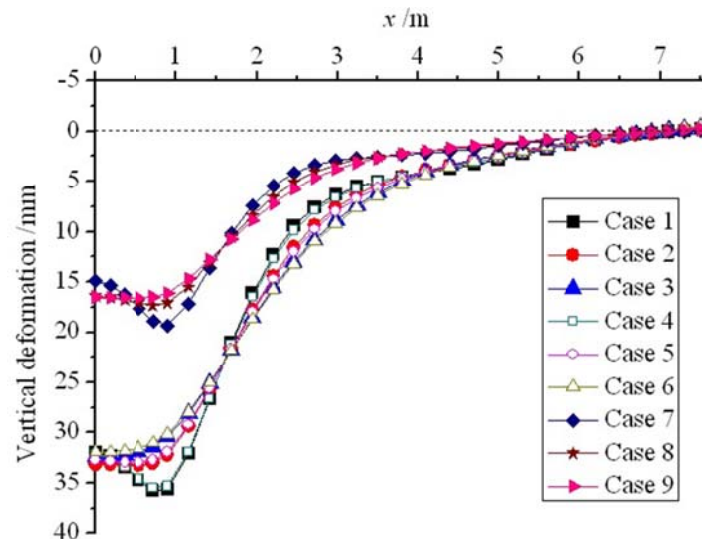Fig. 4 Geocell reinforced embankment in parametric study

Fig. 5 Distribution of vertical deformations along the x-axis in different cases

while the maximum tension force T_{max} within the beam increases with E increases. Taking w_{max} and T_{max} in cases 1 to 3 for example, when E increases from 50 MPa, 150 MPa to 300 MPa, w_{max} decreases from 35.9 mm, 33.3 mm to 32.3 mm, while T_{max} increases from 13.9 kN, 17.1 kN, to 20.8 kN.

From Figs. 5 to 6, it also can be found that, when other calculation parameters keep constants, the maximum vertical deformation w_{max} decreases slightly with the increase of the ratio of k_{ux}/k_{dx}, while the maximum tension force T_{max} within the beam increase significantly with the increase of the ratio of k_{ux}/k_{dx}. Compared the results in case 2 with the results in case 4, w_{max} decreases from 33.3 mm to 32.9 mm, while T_{max} increases from 17.1 kN to 32.8 kN.

It also can be observed from Figs. 5 and 6 that the maximum vertical deformation w_{max} and the maximum tension force T_{max} within the beam decrease with k_z increases. Compared the results in case 2 with the results in case 8, w_{max} decreases from 33.3 mm to 17.4 mm, and T_{max} decreases from 17.1 kN to 14.6 kN. The reductions of w_{max} and T_{max} are 47.7% and 14.6%, respectively.

Table 7 Soil reaction coefficients and beam elastic modulus in the parametric study

	Case 1	Case 2	Case 3	Case 4	Case 5	Case 6	Case 7	Case 8	Case 9
k_z (kN/m^3)	5000	5000	5000	5000	5000	5000	10000	10000	10000
k_{ux} / k_{dx}	2	2	2	4	4	4	2	2	2
E (MPa)	50	150	300	50	150	300	50	150	300

Then, it can be said that, for softer soil foundations, more tension forces within the geocell reinforcements are contributed to reduce the embankment settlements.

6. Conclusions

A decoupled iterative method to assess the deformation behavior of a geocell mattress subjected to symmetrical loads was proposed by modeling the mattress as a supported beam resting on an elastic foundation. The horizontal beam-soil interfacial shear resistances were taken into account in the elastic foundation model. The decoupled iterative method was used to obtain final solutions of the deformations and internal forces including the horizontal and vertical deformations, rotation angle, bending moment, shear force and tension force of the reinforcement. The validity of the proposed solutions was verified by comparing the results with those of existing FEM solutions and power-series solutions.

A parametric study was conducted to study the effect of the soil reaction coefficients and equivalent elastic modulus of the beam on the beam behavior. The results indicated that the maximum vertical deformation of the beam reduces with the increase of the beam elastic modulus and the increase of the vertical soil coefficient, while the maximum tension force within the beam reduces with the increases of the vertical soil coefficient, but increases with the increase of the beam elastic modulus and the increase of the ratio of the soil coefficient on the beam top side to that on the beam bottom side.

It needs to be pointed out that the geocell mattress and the soil below were all treated as linear, elastic materials in current solutions. In application of larger deformation, the solution presented in this study may not be adequate. However, the presented decoupled iterative method is easy to be extended to solve the problem involving large deformations and this will be discussed in another paper. Moreover, the current analytical model is complicated and more work is needed in future studies before implementation in regular designs.

Acknowledgements

References

Arici, M. (1985), "Analogy for beam-foundation elastic systems", *Journal of Structural Engineering*, **111**(8),

1691-1702.

Bourdeau, P.L. (1989), "Modeling of membrane action in a two-layer reinforced soil system", *Computers and Geotechnics*, **7**(1-2), 19-36.

Bowles, J.E. (1996), *Foundation Analysis and Design*, 5th Ed., Mc Graw-Hill Book Company, New York.

Dash, S.K., Rajagopal, K. and Krishnaswamy, N.R. (2007), "Behavior of geocell reinforced sand beds under strip loading", *Canadian Geotechnical Journal*, **44**(7), 905-916.

Dash, S.K., Sireesh, S. and Sitharam, T.G. (2003), "Model studies on circular footing supported on geocell reinforced sand underlain by soft clay", *Geotextiles and Geomembranes*, **21**(4), 197-219.

Edgar, T.V., Puckett, J.A., Sherman, W.F. and Groom, J.L. (1987), "Utilizing geotextiles in highway bridge approach embankments", *Geotextiles and Geomembranes*, **5**(1), 3-16.

Filonenko-Borodich, M.M. (1940), "Some approximate theories of the elastic foundation", *Uchenyie Zapiski Moskogo Gosudarstvennogo Universiteta*, Mekhanica, **46**, 3-18. (in Russian)

Han, J., Oztoprak, S., Parsons, R.L. and Huang, J. (2007), "Numerical analysis of foundation columns to support widening of embankments", *Computers and Geotechnics*, **34**(6), 435-48.

Hetenyi, M. (1946), *Beams on Elastic Foundations*, University of Michigan Press, Ann Arbor, Michigan.

Hua, F. (2003), "Using of wind-drift sand in road pavement", *A thesis presented to the graduate school of the University of Chang'an in partial fulfillment of the requirements for the degree of master of engineering*. (in Chinese)

Latha, G.M., Rajagopal, K. and Krishnaswamy, N.R. (2006), "Experimental and theoretical investigations on geocell-supported embankments", *International Journal of Geomechanics*, **6**(1), 30-35.

Krishnaswamy, N.R., Rajagopal, K. and Madhavi, L.G. (2000), "Model studies on geocell supported embankments constructed over soft clay foundation", *Geotechnical Testing Journal*, ASTM, **23**(1), 45-54.

Ghosh, C. and Madhav, M.R. (1994), "Reinforced granular fill-soft soil system: confinement effect", *Geotextiles and Geomembranes*, **13**(5), 727-741.

Ma, F. and Ai, Z.Y. (2002), "The finite element method of elastic subgrade beam with the contact friction effect considered", *Rock and Soil Mechanics*, **23**(1), 93-96. (in Chinese)

Madhira, R.M. and Hormoz, B. (1988), "A new model for geosynthetic reinforced soil", *Computers and Geotechnics*, **6**(4), 277-290.

Maheshwari, P., Basudhar, P.K. and Chandra, S. (2006), "Modeling of beams on reinforced granular beds", *Geotechnical and Geological Engineering*, **24**(2), 313-324.

Shahira, H. and Pak, A. (2010), "Estimating liquefaction-induced settlement of shallow foundations by numerical approach", *Computers and Geotechnics*, **37**(3), 267-79.

Shukla, S.K. and Chandra, S. (1994), "A study of settlement response of a geosynthetic-reinforced compressible granular fill-soft soil system", *Geotextiles and Geomembranes*, **13**(9), 627-639.

Tan, Z.M. (1997), "Solution method for beam with horizontal resistance on elastic foundation", *Mechanics and Practice*, **19**(3), 33-35. (in Chinese)

Xie, Y.L., Yu, Y.H. and Yang, X.H. (2004), "Application study of treating differential settlement of subgrade with geocell", *Chinese Journal of Highway and Transport*, **17**(4),7-10. (in Chinese)

Yin, J.H. (2000), "Comparative modeling study of reinforced beam on elastic foundation", *Journal of Geotechnical and Geoenvironmental Engineering*, **126**(3), 265-271.

Yin, J.H. (2000), "Closed-form solution for reinforced Timoshenko beam on elastic foundation", *Journal of Engineering Mechanics*, **126**(8), 868-874.

Zhang, L., Zhao, M.H., Zou, X.W. and Zhao, H. (2009), "Deformation analysis of geocell reinforcement using Winkler model", *Computers and Geotechnics*, **36**(6), 977-983.

Zhang, L., Zhao, M.H., Zou, X.W. and Zhao, H. (2010a), "Analysis of geocell reinforced mattress with consideration of horizontal-vertical coupling", *Computers and Geotechnics*, **37**(6),748-756.

Zhang L., Zhao M.H., Shi C.J. and Zhao H. (2010b), "Bearing capacity of geocell reinforcement in embankment engineering", *Geotextiles and Geomembranes*, **28**(2), 475-782.

Zhou, H.B. and Wen, X.J. (2008), "Model studies on geogrid- or geocell-reinforced sand mattress on soft soil", *Geotextile and Geomembranes*, **26**(3), 231-238.